Available online at www.sciencedirect.com
ScienceDirect
International Journal of Mass Spectrometry 255–256 (2006) 144–149
International Journal of Mass Spectrometry
www.elsevier.com/locate/ijms

Impact of ion magnetron motion on electron capture dissociation Fourier transform ion cyclotron resonance mass spectrometry

Yury O. Tsybin [a], Christopher L. Hendrickson [a,1], Steven C. Beu [b], Alan G. Marshall [a,*,1]

[a] *Ion Cyclotron Resonance Program, National High Magnetic Field Laboratory, Florida State University, 1800 E. Paul Dirac Drive, Tallahassee, FL 32310-4005, USA*
[b] *S.C. Beu Consulting, 12449 Los Indios Trail, Austin, TX 78729, USA*

Received 15 November 2005; accepted 16 November 2005
Available online 7 February 2006

Abstract

Electron capture dissociation (ECD) efficiency in a 9.4 T Fourier transform ion cyclotron resonance (FT-ICR) mass spectrometer varies periodically with the time interval between ion and electron injection. The observed modulation frequency correlates to within 1% with ion magnetron frequency, most probably due to misalignment between the ion beam and the electron beam. The optimum ECD conditions are obtained by correctly phasing electron injection with the ion magnetron motion. Displacement of the trapped ion cloud by variation of the ICR trap radial electric field decreases ECD efficiency modulation amplitude. Experiments directly suggest that only ions interacting with electrons at the moment of electron injection participate in ECD reactions.
© 2006 Elsevier B.V. All rights reserved.

Keywords: Electron capture dissociation; Electrospray; Fourier transform; Ion cyclotron resonance; Magnetron motion

1. Introduction

Electron capture dissociation (ECD) in Fourier transform ion cyclotron resonance mass spectrometry (FT-ICR MS) is one of the most prominent methods for complete peptide and protein structural characterization [1–3]. Despite numerous theoretical and experimental attempts to reveal the mechanism of ECD [4,5] and increase fragment ion yield [6–8] biological applications would benefit from further improvement of ECD efficiency. Secondary fragmentation and neutralization of primary fragments are considered the main limitations of ECD efficiency [6].

A recent study of ECD efficiency suggested that electrons in the ICR trap modify ion motion in a way that prohibits ion rotation into the electron beam [9]. That hypothesis is built upon a common experimental observation that only a fraction of the precursor ion population is amenable to ECD. ECD efficiency can reputedly be improved by on- and off-resonance ion excitation prior to electron injection [7] or by sidekick manipulation of ion magnetron motion [10]. However, the direct impact of ion magnetron motion on ECD efficiency has not been reported.

With few exceptions, both ion and electron injection into ICR ion traps are performed on the cylindrically symmetrical magnetic field axis (traditionally called the z-axis) [11,12]. Ion magnetron radii should then be small so that ions are close to the z-axis of the ICR trap, which is assumed to be perfectly aligned with the magnetic field axis. Implementation of a wide electron beam for ECD increases the possibility that the electron beam completely overlaps the ion cloud [8]. However, small shifts in both ion and electron beams from the z-axis are unavoidable, so that the overlap between ions and electrons is incomplete, and ion magnetron motion can modulate the overlap. As a result, efficiencies of ECD with a hollow electron beam of more than 1 mm inner diameter and a pencil electron beam are comparable [12].

In this work, we show that ECD efficiency varies periodically with ion magnetron motion. The parameters of the observed dependence are investigated and ways to decrease the ECD efficiency amplitude are explored. The experimental

* Corresponding author. Tel.: +1 850 644 4595/0539; fax: +1 850 644 8281/1366.
E-mail address: marshall@magnet.fsu.edu (A.G. Marshall).
[1] Member of the Department of Chemistry and Biochemistry, Florida State University, Tallahassee, FL 32306, USA.

1387-3806/$ – see front matter © 2006 Elsevier B.V. All rights reserved.
doi:10.1016/j.ijms.2005.11.014

evidence supports the hypothesis that ECD fragments are generated only from precursor ions that overlap with the electron beam at the instant of electron injection. Finally, improved ECD efficiency for two consecutive ion isolation/ECD events is demonstrated.

2. Methods

2.1. Sample preparation

Standard peptides, proteins and formic acid were purchased from Sigma (St. Louis, MO) and used without further purification. Acetonitrile and water (HPLC grade) were purchased from J.T. Baker (Philipsburg, NJ). For electrospray, aqueous stock solutions were diluted to a concentration of 1 μM in 50/50 vol% acetonitrile: water with 0.1% (v/v) formic acid.

2.2. Fourier Transform ion cyclotron resonance mass spectrometry

Mass analysis was performed with a homebuilt 9.4 T ESI-Q-FT-ICR mass spectrometer equipped with a dispenser cathode-based electron gun for ECD experiments [11]. Microelectrospray was employed with a flow rate of ∼300 nL/min [13]. After 0.1–5 s accumulation in the external octopole ion trap (4.8 mm i.d., 15 cm long, 300 V_{p-p} at 1.5 MHz), ions were transported by a radiofrequency octopole ion guide (4.8 mm i.d., 160 cm long, 125 V_{p-p} at 1.5 MHz) into an open ended cylindrical ICR trap (94 mm i.d., 300 mm long). Gated ion trapping was employed without cooling gas. Trapped ions acquired the characteristic magnetron frequency (determined by the magnetic field strength, ICR trap geometry and applied trap potential (1–10 V)) during a 100 ms delay. The coherence of the ion cloud magnetron motion is most probably a consequence of the short (compared to one magnetron cycle) duration of ion injection period into the ICR cell, namely, ∼100 μs for ions of one *m/z* value. A second, variable period was incorporated afterward to investigate the effect on ECD efficiency. Subsequently, a 3 mm diameter electron beam (1–100 ms) was injected into the ICR trap followed by an electron clean-up event (100 ms) [9]. Ions were allowed to cool for 300 ms prior to excitation and detection. The cathode potential during electron injection was −5 V and kept at +10 V otherwise. Precursor ion selection was performed in the external quadrupole mass filter [14] or in the ICR trap by stored waveform inverse Fourier transform (SWIFT) excitation [15]. Prior to broadband detection (818 ms detection period, 512 Kword data points) ions were frequency-sweep excited (72–720 kHz at 150 Hz/μs). The standard procedure to obtain a mass-to-charge ratio mass spectrum was employed [9]. Briefly, the time-domain transient signal was baseline corrected, Hanning apodized, zero filled and Fourier transformed to produce a magnitude-mode frequency spectrum that was finally converted to a mass-to-charge ratio spectrum by the quadrupolar approximation [16]. Data acquisition was performed by use of a Predator data station and data analysis with MIDAS 2.7 Software [17].

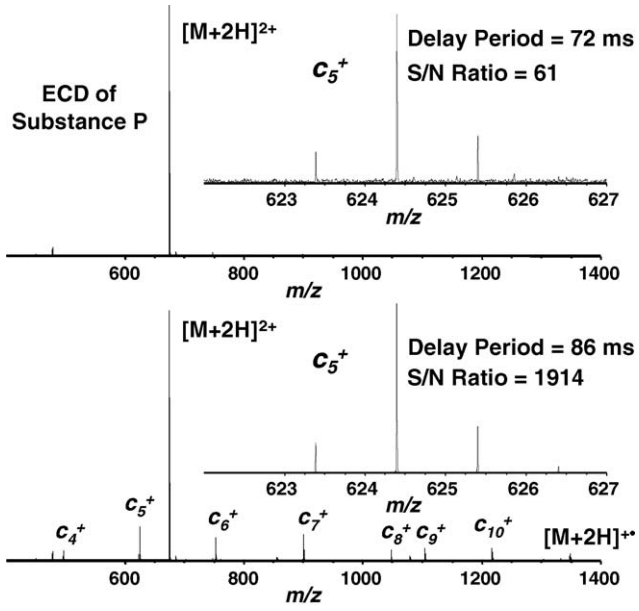

Fig. 1. ECD FT-ICR mass spectra (each from four summed time-domain transients) of substance P acquired after an ion relaxation period between ion trapping and electron injection into the ICR trap of: (a) 72 ms and (b) 86 ms. Electron irradiation period is 100 ms. ICR trap voltage is 10 V.

3. Results and discussion

3.1. ECD efficiency modulation

Electron capture dissociation (ECD) efficiency exhibited a periodic dependence on the delay period between ion trapping and electron injection into the ICR trap, for different standard peptide (Fig. 1) and protein (Fig. 2) ions. The variation in ECD

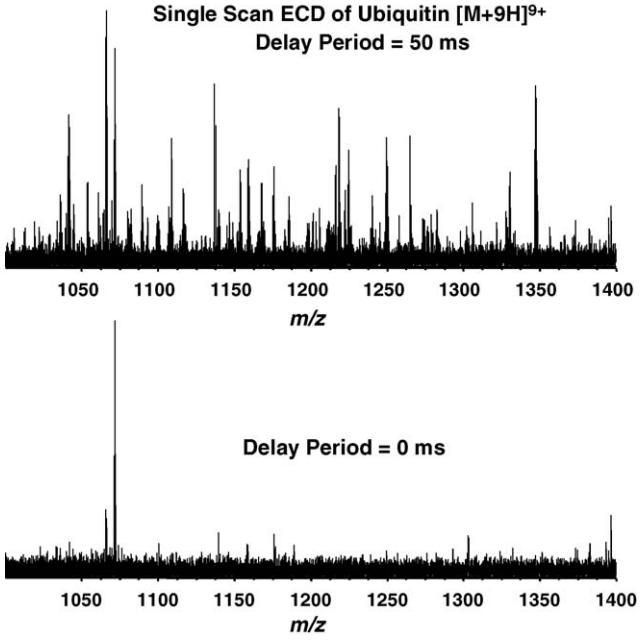

Fig. 2. Single scan ECD FT-ICR MS of ubiquitin $[M+9H]^{9+}$, demonstrating a strong dependence on delay period between ion trapping and electron injection. Electron irradiation period is 10 ms. ICR trap voltage is 5 V.

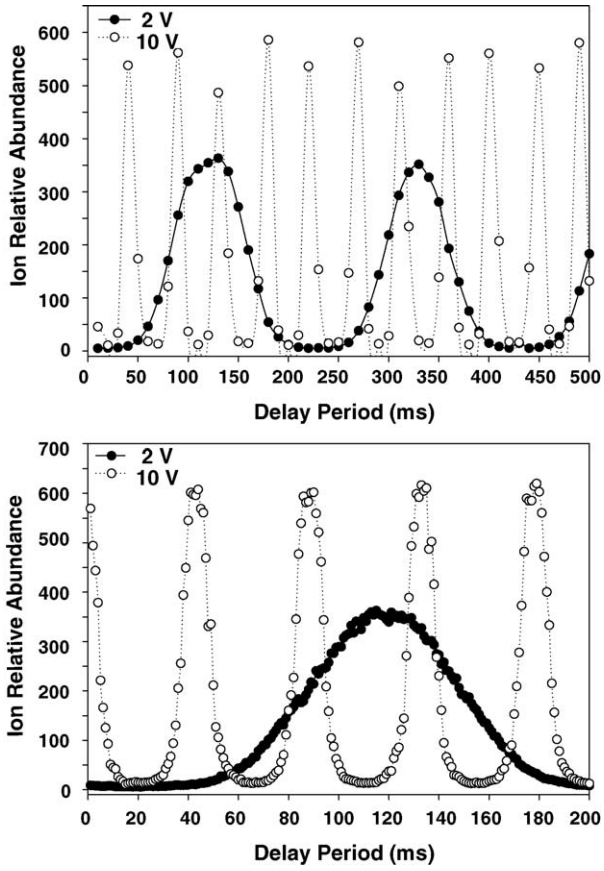

Fig. 3. ECD fragment ion abundance as a function of delay period between ion trapping and electron injection. Trap electrode potentials are 2 V (●) and 10 V (○). The ion relaxation period increment was (top) 10 ms and (bottom) 1 ms.

fragment ion abundance within one period was more than an order of magnitude (Fig. 1 insets and Fig. 2). Precursor ion signal acquired without electron injection under otherwise identical experimental conditions shows only minor (within 5% scan-to-scan) amplitude variation, presumably due to spray instability (data not shown). The periodic dependence of ECD fragment ion abundance as a function of delay period for different ion trapping potentials for doubly charged substance P ions ($m/z = 674$) is shown in Fig. 3. The electron injection period was 1 ms, and the delay period was varied by increments of 10 ms (Fig. 3, top) and 1 ms (Fig. 3, bottom).

3.2. Effect of ICR trapping potential

The period of ECD efficiency modulation (Fig. 3) was found to be about 44 ms for 10 V trap potentials and about five times longer with 2 V. The corresponding 22 Hz modulation frequency matches (to 1% accuracy) the calculated magnetron frequency obtained by SIMION modeling of the employed experimental conditions. The expected linear (with linearity factor $R^2 = 0.9993$) dependence of ECD modulation frequency on the trap potentials (Fig. 4) confirms that magnetron motion induces modulation of ECD efficiency.

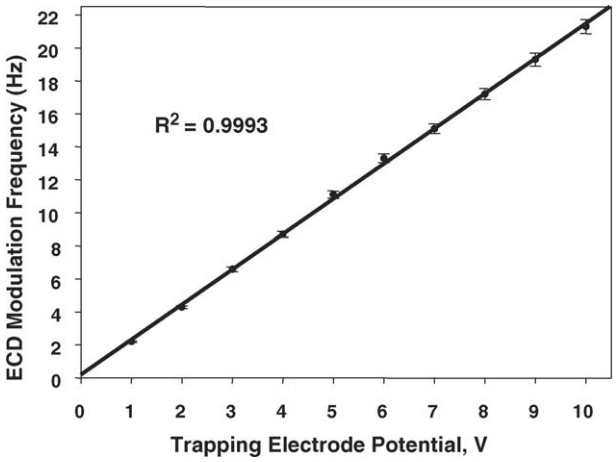

Fig. 4. ECD efficiency modulation frequency as a function of applied trap electrode potential. The straight line is the calculated magnetron frequency for the ICR cell geometry and applied magnetic field strength.

3.3. Effect of ion number

For sufficiently low ion number (signal/noise ratio of doubly charged precursor ions is ~1000), the variation of ECD efficiency with delay period is almost negligible. Increasing the number of ions resulted in narrower ECD modulation peak width (full width at half maximum peak height) and increased amplitude of ECD variation within one period (Fig. 5). For the present ion numbers, a maximum ECD efficiency variation of about 30-fold was obtained. The gain was calculated as the ratio of maximum to minimum total fragment ion abundance (Figs. 3 and 5):

$$\text{Gain}_{\text{ECD efficiency}} = \frac{\sum(\text{fragment ion abundance})|_{\max}}{\sum(\text{fragment ion abundance})|_{\min}} = \frac{\sum(\text{fragment ion abundance})|_{\max}/\text{precursor ion abundance}}{\sum(\text{fragment ion abundance})|_{\min}/\text{precursor ion abundance}} = \frac{\text{efficiency}|_{\max}}{\text{efficiency}|_{\min}} \quad (1)$$

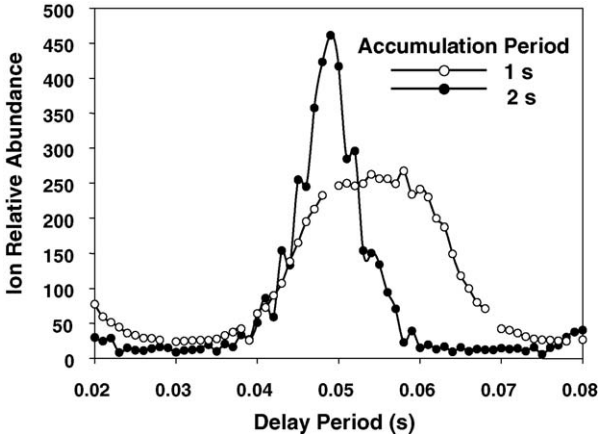

Fig. 5. Dependence of ECD product ion modulation amplitude on the number of trapped ions: (○, 1s ion accumulation period (lower ion number)); (●, 2s accumulation period (higher ion number)).

The observed dependence suggests that increased ion density contributes to the initial magnetron radius of the ion cloud. As a consequence, changes in magnetron motion parameters change the optimum delay period for maximum ECD efficiency. Therefore, the delay period should be adjusted according to the number of injected ions. The maximum ion number achieved did not reach the upper limit of ICR trap capacity. The difference between the minimum and maximum ion number studied was about two orders of magnitude. Further increase in ion number reduces ECD efficiency. The effect is probably due to an increase in magnetron radius to a value larger than the radius for interaction with the electron beam. It is also possible that lateral displacement of the ion cloud from the z-axis and space charge perturbation of the ion trajectory during passage through the transfer octopole can occur.

3.4. Effect of radial electric field

ECD efficiency modulation suggests that the ICR trap electric field z-axis is not sufficiently aligned with the electron beam (which may not be sufficiently aligned with the magnetic field z-axis). However, the electric z-axis of the trap can be shifted by application of a dc voltage to the trap side electrodes (introducing an additional radial electric field that could realign the ion cloud z-axis with the electron beam). SIMION modeling indicates that a 250 mV potential on a detection electrode shifts the radial potential center of the trap by 1.87 mm if the end cap potentials are 10 V, and by 12.5 mm if the end cap potentials are 2 V. However, the equipotential contours are not concentric about the shifted axis if the boundary values are asymmetric. Therefore, the actual shift in the center of magnetron gyration will depend on the radial amplitude.

We imposed a radial electric field by applying a dc potential to one of the excitation electrodes (with no dc potential applied to the opposite plate). Application of a dc potential in a direction (x- or y-) transverse to the z-axis was performed by switching pairs of excitation and detection electrodes while applying the dc potential to one of the detection side electrodes in both cases.

The subsequent change in the ECD fragment ion abundance as a function of applied dc potential is shown in Fig. 6 (closed circles). First, the delay period between ion trapping and electron injection was chosen such that ECD efficiency was close to its minimum in the absence of application of a transverse dc potential. Application of dc potential to one pair of side electrodes (labeled "y") did not significantly increase ECD fragment ion abundance Fig. 6 (closed circles). However, an order of magnitude increase in ECD efficiency was achieved by applying a 100–300 mV negative potential to the other pair of side electrodes (Fig. 6, open circles), with an optimum ECD yield at −250 mV dc potential. In the latter case a 5 ms shorter delay period prior to electron injection was employed.

After application of a −250 mV potential to the side electrodes to displace the ion beam relative to the electron beam, periodic modulation of the ECD fragment ion abundance modulation with delay periods remains (Fig. 7, closed circles), but with phase inverted relative to the modulation observed in the absence of the applied dc potential. Therefore, the applied potential evidently displaced the ion cloud symmetrically to the opposite side of the electron beam. Therefore, optimal ion cloud overlap with an electron beam should be produced by applying a dc potential between 0 and −250 mV. In support of that conclusion, application of a −128 mV dc potential efficiently reduced the ECD efficiency modulation amplitude while maintaining the average ECD efficiency level close to its maximum value (Fig. 7, open circles). Further reduction in the modulation amplitude could presumably be achieved by simultaneous application of (different) dc potentials to orthogonal side electrodes.

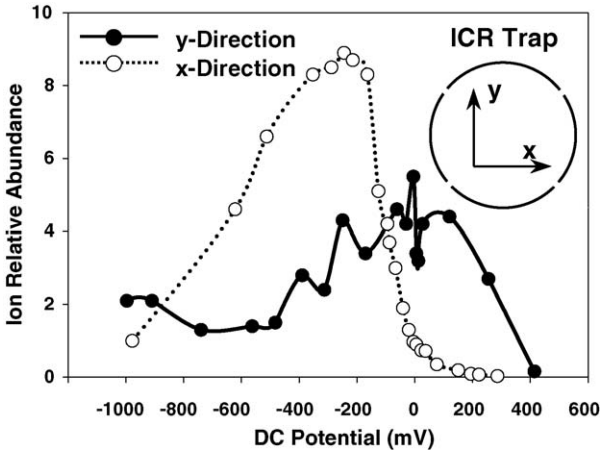

Fig. 6. Influence of dc potential applied to the ICR trap excitation electrodes on the abundance of ECD fragment ions. (●) and (◯) designate different pairs of side electrodes used to shift the ion cloud in each of two dimensions of radial motion (i.e., x- or y-axis).

3.5. Overlap between trapped ion packet and electron beam

Despite an initial attempt to position both electron and ion beams on-axis in the present instrument configuration [11], the present behavior is most probably due to misalignment of either the ion beam or the electron beam relative to the magnetic field symmetry axis. Therefore, trapped ions rotate about the electric

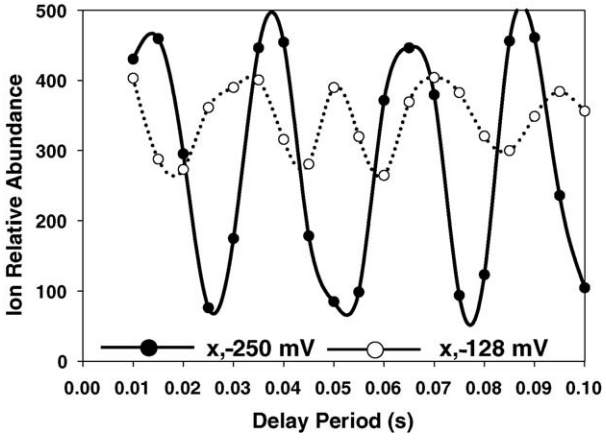

Fig. 7. ECD efficiency modulation as a function of delay period between ion and electron injection with a 128 mV potential difference between the excitation electrodes (◯) or a 250 mV potential difference between the excitation electrodes (●).

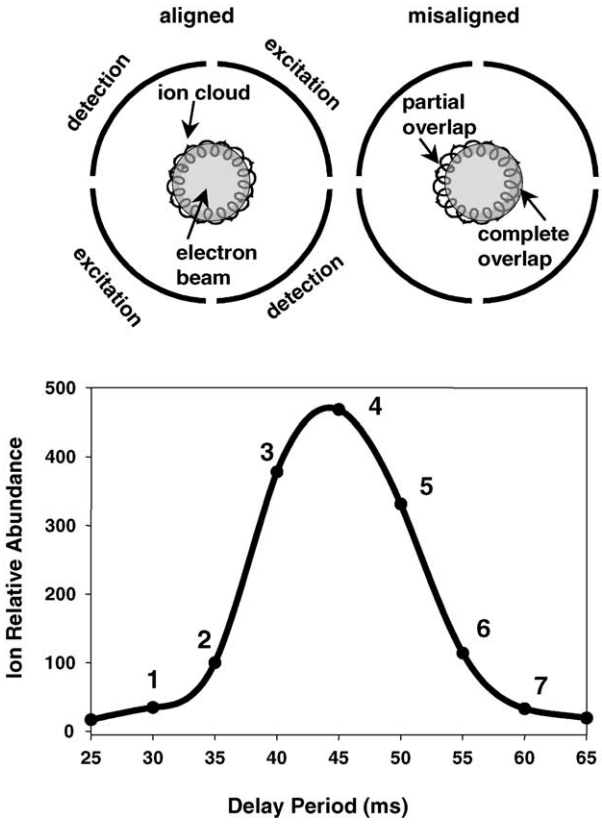

Fig. 8. Schematic representation of overlap between the ion cloud and electron beam shown in transverse cross section. Top left: the ion cloud magnetron axis is collinear with the electron beam. Top right: the electron beam is displaced laterally relative to the ion cloud magnetron axis. Bottom: the observed dependence of ECD fragment ion abundance on electron injection delay period (bottom) correlates well with non-collinear electron beam and magnetron axes.

saddle point of the ICR trap, whereas the center of the electron beam is not perfectly aligned with that point (Fig. 8, top). Asymmetry in the transverse dc electric potential field of the ICR trap could also account for an off-axis shift of the ion cloud and development of the ion magnetron motion. In either case, ion and electron beam alignment by tuning of the transverse dc electric field decreases the ECD efficiency modulation amplitude even for high ion numbers (Figs. 6 and 7).

The maximum ECD efficiency should depend directly on the extent of overlap between electron and ion clouds. A single period of ECD efficiency modulation is shown in Fig. 8, bottom. Correlation with Fig. 8 (upper right) (misaligned electrons and ions) suggests small overlap at points 1, 2, 6 and 7, whereas overlap is much better at points 3–5 at the moment of electron injection. In principle, complete overlap of ions and electrons should result in 100% efficient electron capture.

3.6. Effect of electron irradiation period

The dependence of ECD fragment ion abundance on electron injection period was investigated to test the hypothesis that electrons interact only with ions that overlap at the instant of electron injection [9] (Fig. 9). The theoretical curve derived assuming ions can enter and exit the electron beam as if ion magnetron

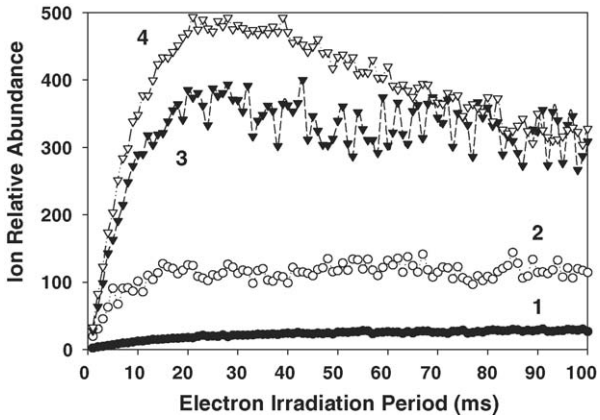

Fig. 9. ECD fragment ion abundance as a function of the electron irradiation period for different intervals between ion trapping and electron injection (denoted in Fig. 8, bottom)).

motion is independent of the presence of electrons demonstrates a periodic dependence with stepwise increase in the abundance of product ions as parent ions periodically rotate into the electron beam (data not shown).

Experimentally, ECD fragment ion abundances were measured as a function of electron irradiation period for four of the injection time points defined in Fig. 8, bottom (data shown in Fig. 9). The increment in the electron irradiation period was 1 ms, i.e., much shorter than the ion magnetron motion period (~45 ms at trapping voltage 10 V). If electrons are injected with poor ion-electron beam overlap (Fig. 9, closed circles, point 1) the ECD fragment ion abundance maximum increased 10 times when the electron irradiation period reached the ion magnetron period. However, the maximum ECD efficiency obtained is only a few %. Prolongation of electron irradiation period resulted in 10–20% increase of ECD fragment ion abundance.

Conversely, electron injection at a time point corresponding to maximum ion-electron beam overlap exhibits higher maximum ECD efficiency value (up to 15–20%). An initial linear increase in ECD fragment ion abundance with increasing delay is followed by a pronounced decrease, presumably due to neutralization of the primarily formed fragments (Fig. 9, open triangles, point 4). Therefore, the magnitude of ECD fragment ion abundance increase in points 1 and 4 are comparable (about 10 times), but larger initial ion-electron beam overlap in point 4 results in much more abundant ECD fragment ions at the maximum. The intermediate states of ion-electron beam overlap are shown in Fig. 9 as closed triangles (point 3) and open circles (point 2). The time delay interval between the points is 5 ms.

The difference between theoretically predicted and experimentally observed (Fig. 9) ECD fragment ion abundance dependence on electron irradiation period confirms that ions do not rotate into the electron beam. Ion trajectories in the presence of an electron beam should exhibit similarity to ion motion in a wire ion guide ICR trap (Kingdon ion trap in a magnetic field) [18,19]. We suspect that the electric field of the electron beam modifies ion trajectories so that they rotate around the electron beam without penetrating it. Efforts to simulate ion motion under the influence of the electron beam are underway.

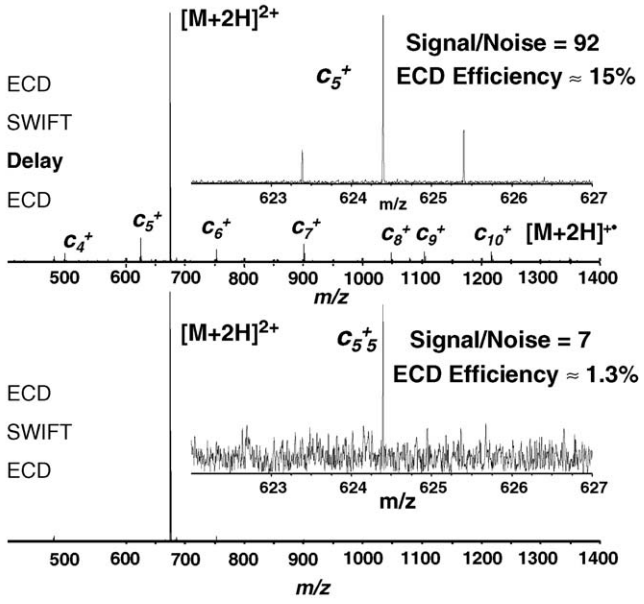

Fig. 10. ECD FT-ICR mass spectra of substance P after SWIFT isolation of precursor ions left after a first ECD event with (top) and without (bottom) a delay of 115 ms between SWIFT isolation and a second electron injection event. The ECD efficiency for the first event (15%) can be reproduced in the second ECD event only with an appropriate delay (see text).

3.7. Improved ECD for SWIFT-isolated precursor ions

Optimization of the delay between ion injection and electron injection also increased the efficiency of two consecutive ion isolation/ECD events. First, an optimized ECD mass spectrum of isolated doubly charged precursor ions was acquired (ECD efficiency was 15%). Second, SWIFT isolation of the remaining precursor ions was performed. Prior to the next ECD event a variable time delay was incorporated. Delay period optimization revealed a strong influence on ECD fragment ion abundance (Fig. 10). The ECD efficiency in the second ECD event reached the same value as in the first ECD event, confirming prior speculation [9] that misalignment of ions and electrons compromises ECD MS^n experiments and contradicting the hypothesis that SWIFT excitation-induced magnetron expansion could be solely responsible for ECD efficiency drop.

4. Conclusion

ECD efficiency modulation is observed and optimal efficiency is achieved by appropriate choice of delay between ion and electron injection. Ion magnetron motion is responsible for the observed modulation. Increased ion number in the ICR trap produces narrower and higher ECD efficiency maxima. Application of a small additional dc radial electric field to the excitation electrodes of the ICR trap can improve the overlap between ions and electrons and decrease the ECD efficiency modulation amplitude.

The presently observed phenomena should be general to both home-built and commercial FT-ICR mass spectrometers. In addition to the above-mentioned mechanical misalignment, influence of the ICR trap electric field, and high ion concentration induced magnetron radii increase, the effect can be induced by magnetron motion expansion by sidekick ion trapping or performing ECD with small diameter electron beams (directly heated filaments, small dispenser cathodes, off-axis dispenser cathodes).

Finally, for different delay periods between ion and electron injection, ECD efficiency does not increase monotonically to the same maximum value with increasing electron irradiation period. Therefore, ions do not rotate into the electron beam, even when the electron irradiation duration exceeds the ion magnetron motion period. Those ions not in the electron beam at the start of irradiation will instead orbit around the beam as the associated electric field now dominates the ion motion.

Acknowledgments

The authors thank Oleg Yu. Tsybin and Melinda A. McFarland for helpful discussions. This work was supported by the NSF National High-Field FT-ICR Mass Spectrometry Facility (CHE 99-09502), Florida State University, and the National High Magnetic Field Laboratory at Tallahassee, Florida.

References

[1] R.A. Zubarev, Mass Spectrom. Rev. 22 (2003) 57.
[2] H.J. Cooper, K. Hakansson, A.G. Marshall, Mass Spectrom. Rev. 24 (2005) 201.
[3] Y.O. Tsybin, M. Ramstrom, M. Witt, G. Baykut, P. Hakansson, J. Mass Spectrom. 39 (2004) 719.
[4] V. Bakken, T. Helgaker, E. Uggerud, Eur. J. Mass Spectrom. 10 (2004) 625.
[5] E.A. Syrstad, F. Turecek, J. Am. Soc. Mass Spectrom. 16 (2005) 208.
[6] M.V. Gorshkov, C.D. Masselon, E.N. Nikolaev, H.R. Udseth, L. Pasa-Tolic, R.D. Smith, Int. J. Mass Spectrom. 234 (2004) 131.
[7] M. Mormann, J. Peter-Katalinic, Rapid Commun. Mass Spectrom. 17 (2003) 2208.
[8] Y.O. Tsybin, P. Hakansson, B.A. Budnik, K.F. Haselmann, F. Kjeldsen, M. Gorshkov, R.A. Zubarev, Rapid Commun. Mass Spectrom. 15 (2001) 1849.
[9] M.A. McFarland, M.J. Chalmers, J.P. Quinn, C.L. Hendrickson, A.G. Marshall, J. Am. Soc. Mass Spectrom. 16 (2005) 1060.
[10] S.V. Rakov, J.H. Futrell, E.V. Denisov, E.N. Nikolaev, Eur. J. Mass Spectrom. 6 (2000) 299.
[11] K. Hakansson, M.J. Chalmers, J.P. Quinn, M.A. McFarland, C.L. Hendrickson, A.G. Marshall, Anal. Chem. 75 (2003) 3256.
[12] Y.O. Tsybin, M. Witt, G. Baykut, F. Kjeldsen, P. Hakansson, Rapid Commun. Mass Spectrom. 17 (2003) 1759.
[13] M.R. Emmett, F.M. White, C.L. Hendrickson, S.D.H. Shi, A.G. Marshall, J. Am. Soc. Mass Spectrom. 9 (1998) 333.
[14] B.E. Wilcox, C.L. Hendrickson, A.G. Marshall, J. Am. Soc. Mass Spectrom. 13 (2002) 1304.
[15] S.H. Guan, A.G. Marshall, Int. J. Mass Spectrom. Ion Processes 158 (1996) 5.
[16] S.D.H. Shi, J.J. Drader, M.A. Freitas, C.L. Hendrickson, A.G. Marshall, Int. J. Mass Spectrom. 196 (2000) 591.
[17] G.T. Blakney, T.T. Lam, C.L. Hendrickson, A.G. Marshall, The 52nd ASMS Conference on Mass Spectrometry and Allied Topics, Amer. Soc. Mass Spectrom., Nashville, Tennessee, USA, 2004.
[18] K.J. Gillig, B.K. Bluhm, D.H. Russell, Int. J. Mass Spectrom. Ion Processes 158 (1996) 129.
[19] R.R. Lewis, J. Appl. Phys. 53 (1982) 3975.